Supplementary Information

A Structural Color Hydrogel for Diagnosis of Halitosis and Screening of Periodontitis

Chuanshun Hu, Jieyu Zhou, Jin Zhang, Yonghang Zhao, Chunyu Xie, Wei Yin, Jing Xie, Huiying Li, Xin Xu, Lei Zhao, Meng Qin, and Jianshu Li**

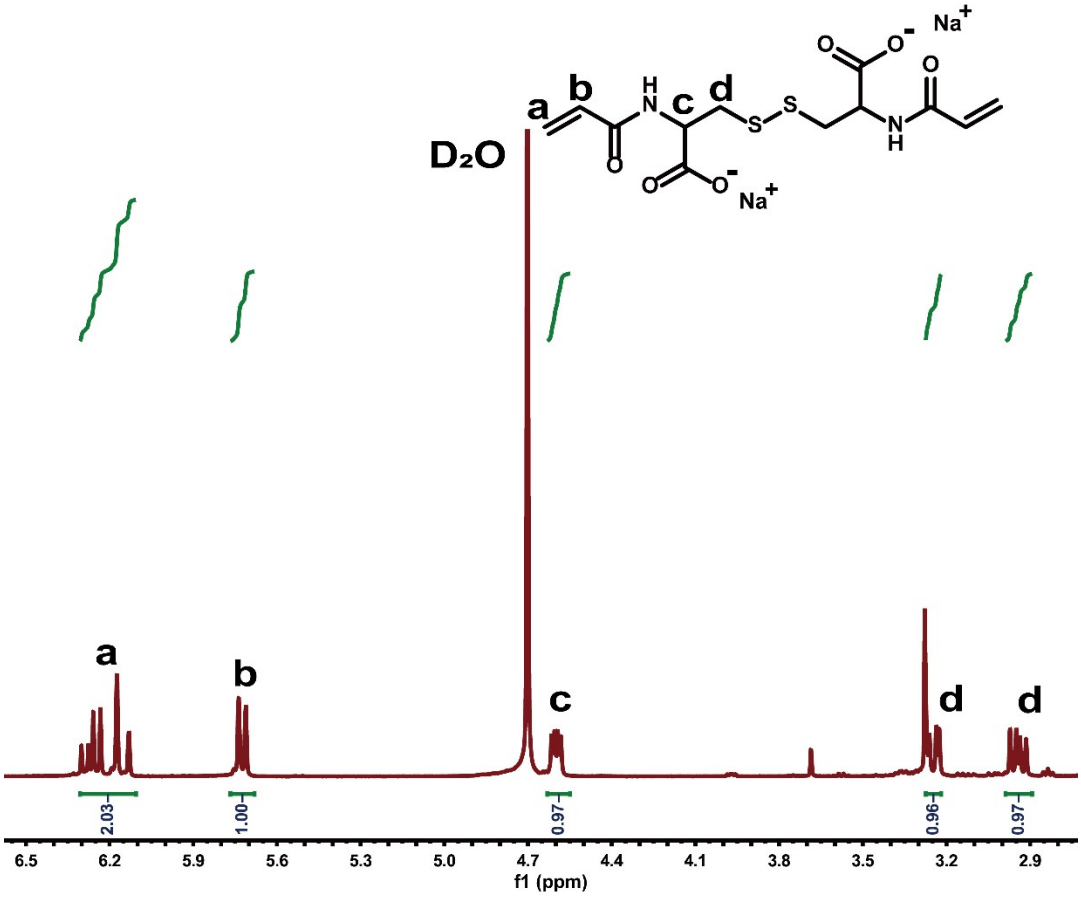

Figure S1. ^{1}H NMR (solvent: D_2O 400 MHz) spectrum of the disulfide crosslinker BISS.

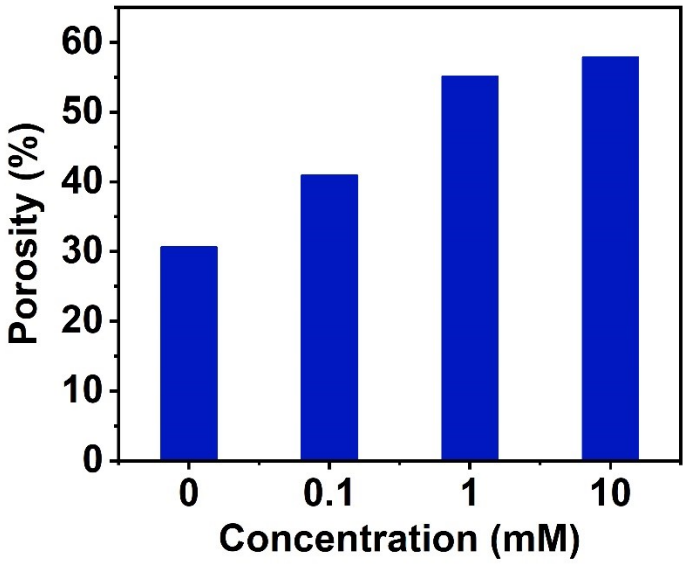

Figure S2. Changes in hydrogel porosity after incubating with different concentrations of Na_2S solutions.

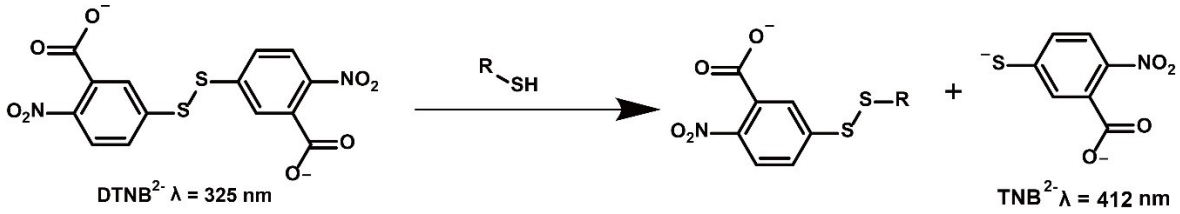

Figure S3. Mechanism of sulfhydryl groups detection with DTNB.

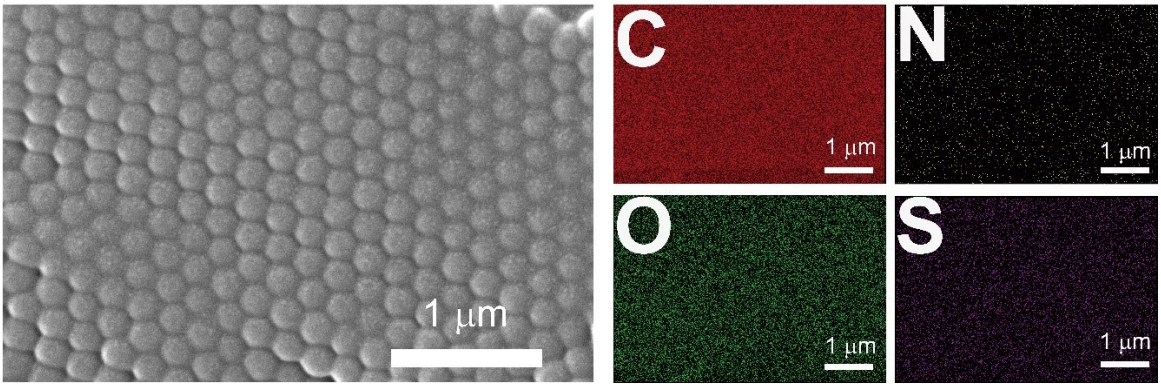

Figure S4. SEM and EDS images of the structural color hydrogels.

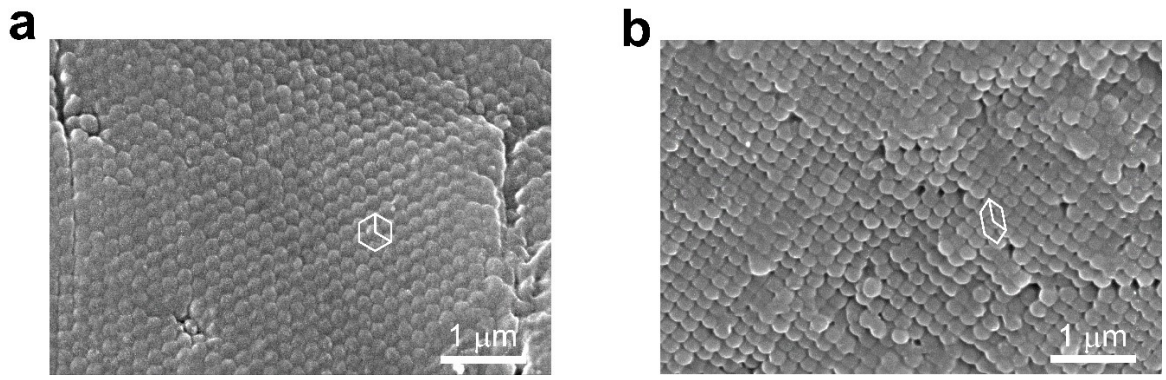

Figure S5. Cross-section images of the structural color hydrogel before (a) and after (b) reduction by Na_2S solution.

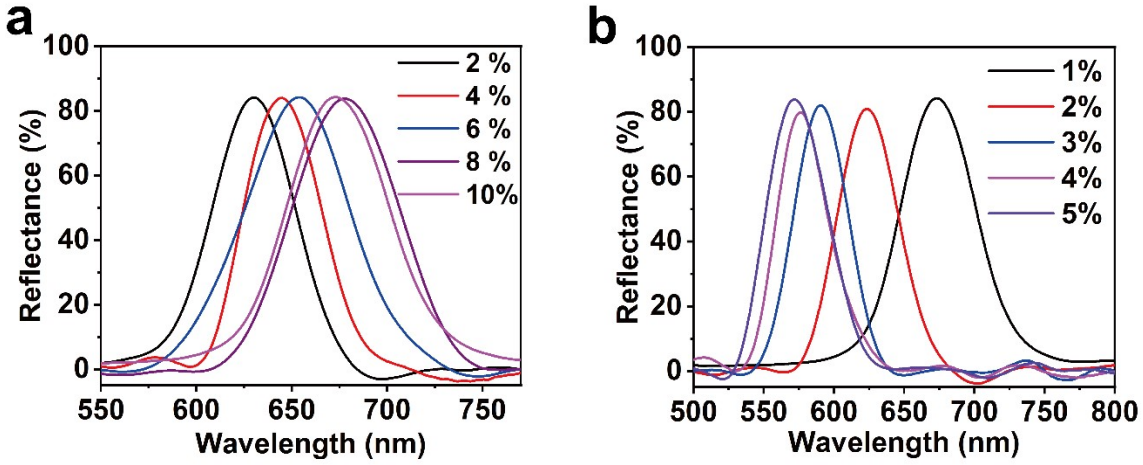

Figure S6. Reflectance spectra of structural color hydrogels with (a) different molar ratios of BISS to AAm and (b) different molar ratios of BIS to AAm.

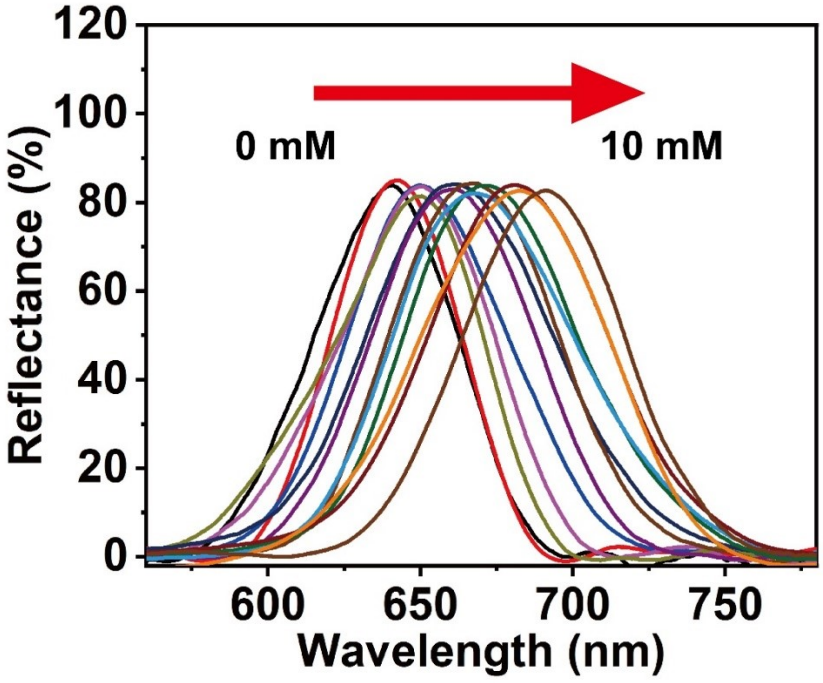

Figure S7. Reflectance spectra of the structural color hydrogel in the presence of different concentrations of Na_2S solutions.

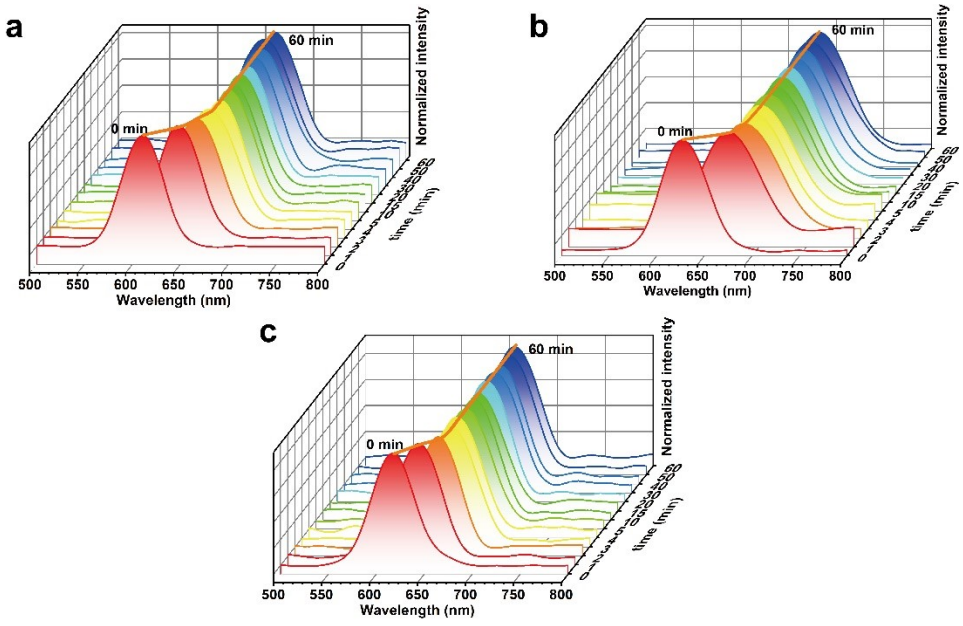

Figure S8. Time-dependent reflectance spectra of the structural color hydrogels responding to varying concentrations of Na_2S. (a) 1.0 mM, (b) 0.5 mM, (c) 0.1 mM.

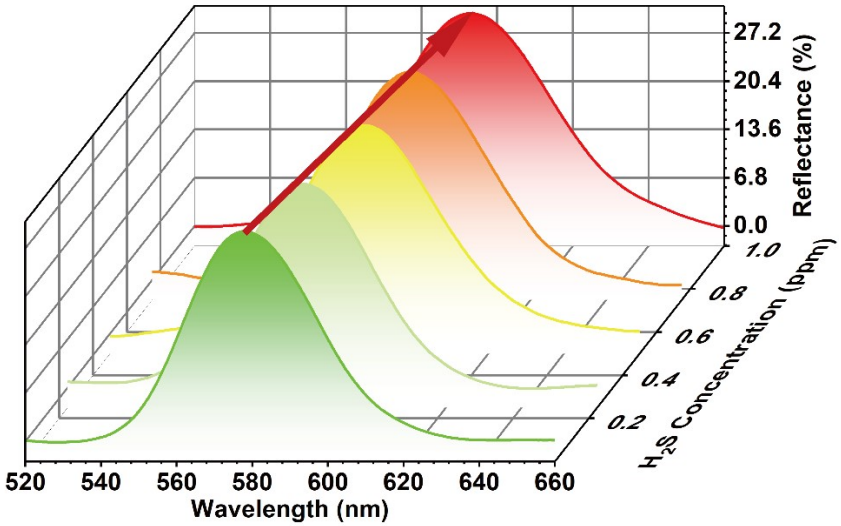

Figure S9. Reflectance spectra of the structural color hydrogel with H_2S concentration increased from 0 to 1 ppm.

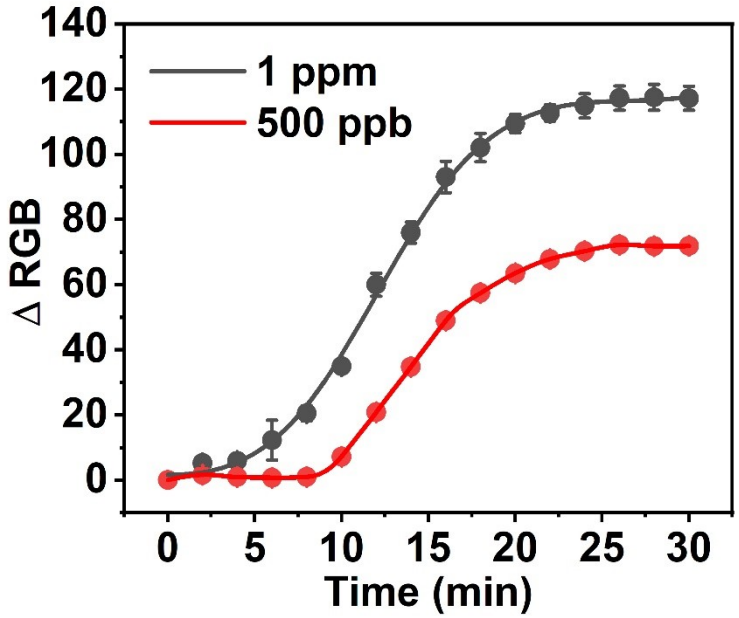

Figure S10. Diffusion kinetics of H_2S in the hydrogel by investigating time-dependent color change of the hydrogel.

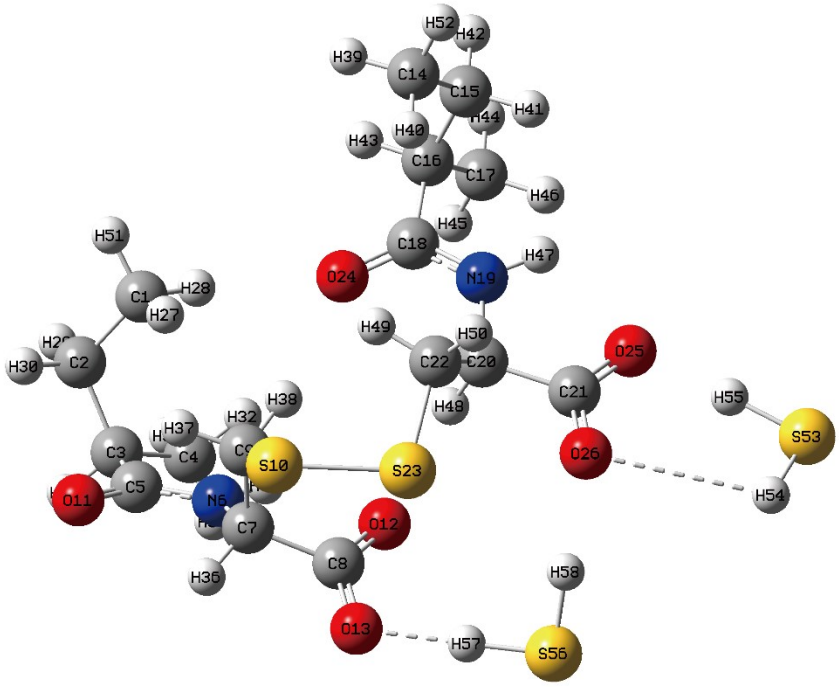

-19.33 Kcal/mol

Figure S11. The binding energy between H_2S and BISS repeating unit. The binding energy is -19.33 Kcal/mol.

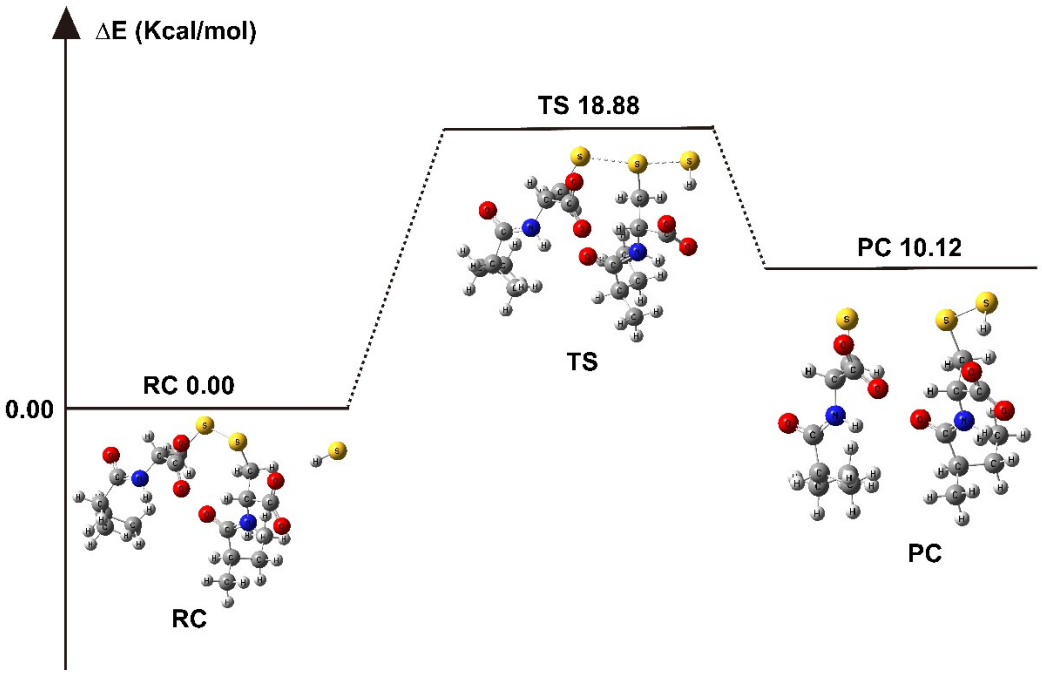

Figure S12. Potential energy profiles of pre-reactive compounds (RC), transition states (TS) and post-reactive compounds (PC) during the reaction between H_2S and disulfide bonds. The energy barrier for this reaction is 18.88 Kcal/mol.

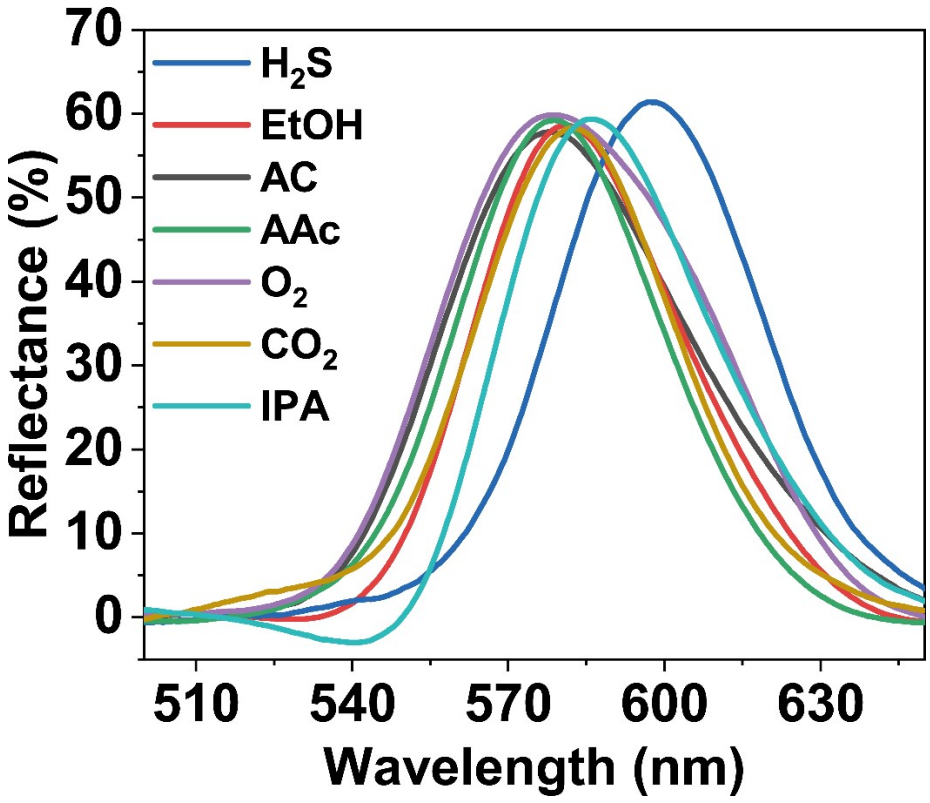

Figure S13. Reflectance spectra of the structural color hydrogel in response to different gases. Gas concentrations are all controlled at 1 ppm.

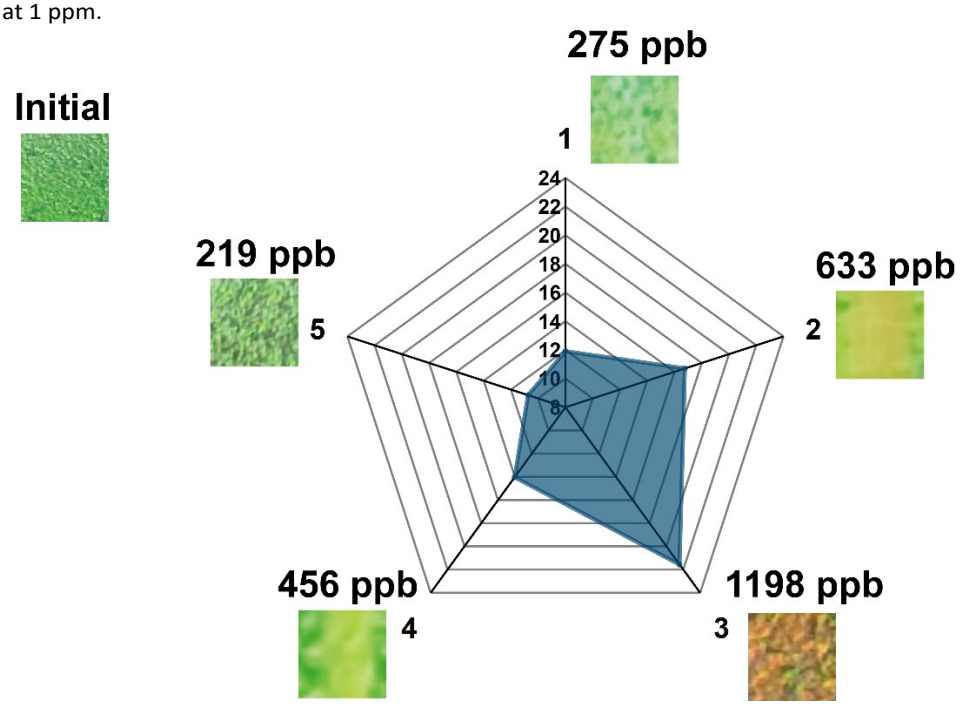

Figure S14. Detection of VSCs in breath samples of patients with halitosis. Radar plot shows the bandgap shift of the structural color hydrogels in response to the samples.

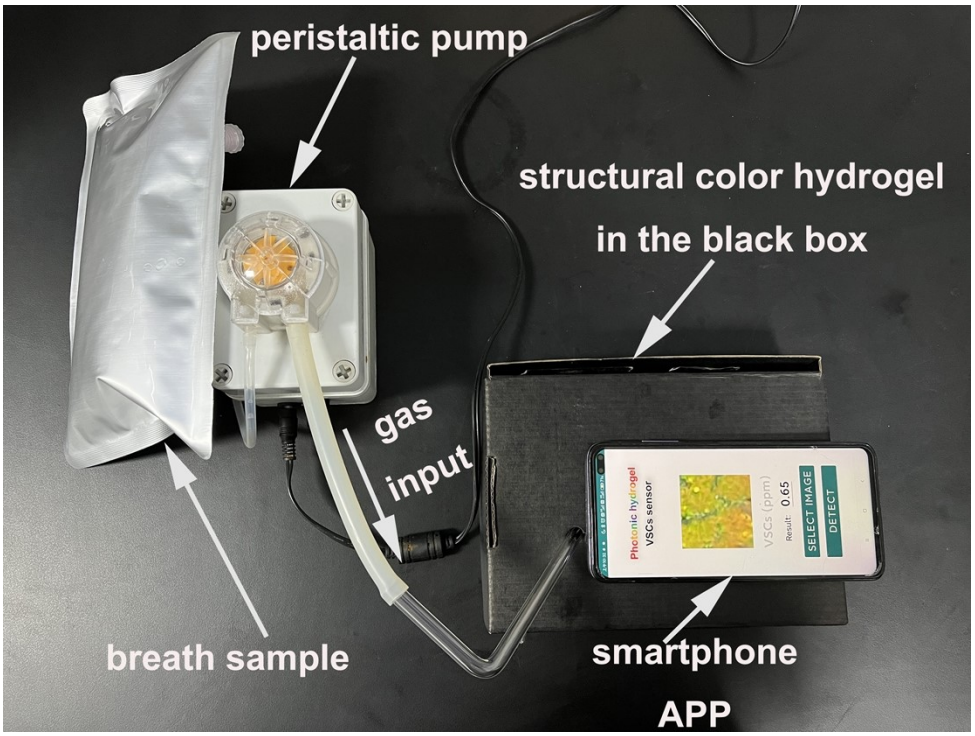

Figure S15. Detection device for smartphone-based detection of VSCs.

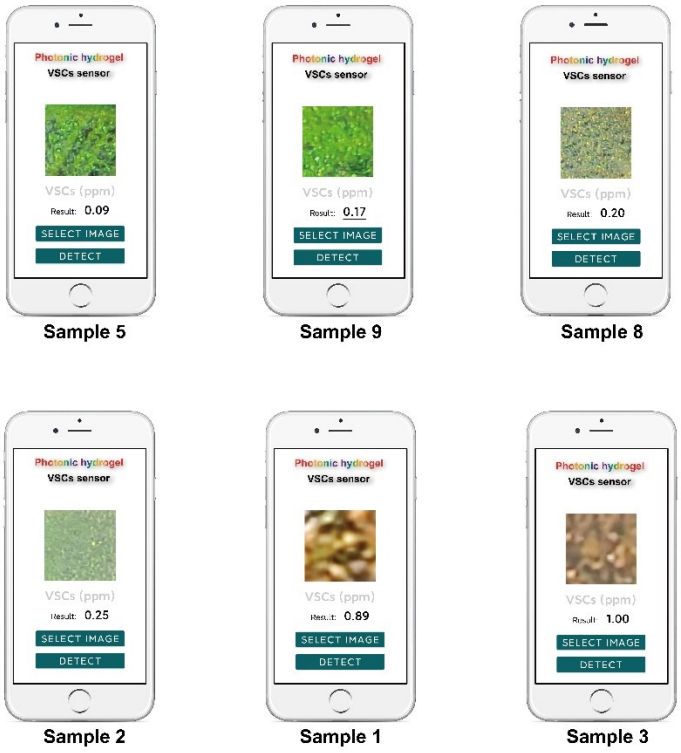

Figure S16. Screenshots of results of detecting VSCs in clinical samples.

Table S1. Quantitative detection of VSCs in clinical samples by the structural color hydrogel. The result is consistent with the clinical diagnosis by the commonly used Halimeter.

Sample number	Mean bandgap shift	structural color hydrogel test results (ppb)	Halimeter test results (ppb)
1	11.91	304	275
2	16.77	698	633
3	21.56	> 1000	1198
4	14.03	477	456
5	10.75	210	219

Table S2. RGB values of the sensor array after responding to clinical samples.

Sample number	VSCs Concentration (ppb)	S1			S2			S3		
		R	G	B	R	G	B	R	G	B
1	880	227.482	142.582	92.092	134.346	173.086	179.304	152.219	141.834	156.787
2	225	184.463	212.092	156.442	158.596	147.376	184.402	180.985	159.635	177.309
3	1231	223.702	123.606	90.451	156.726	184.531	171.248	156.228	130.628	156.940
4	857	226.589	152.338	96.998	125.280	161.313	179.812	157.941	118.374	150.415
5	58	167.906	223.415	140.283	135.329	156.107	175.561	207.562	152.536	161.780
6	684	221.335	211.518	138.529	115.260	113.731	208.808	161.324	133.368	100.576
7	223	186.920	213.510	164.280	164.089	143.217	190.759	185.384	154.277	171.292
8	209	148.544	222.143	167.171	166.017	151.383	180.456	184.726	153.702	170.953
9	120	145.854	221.215	130.487	149.241	159.022	170.845	183.017	158.034	168.427

Table S3. Eigenvalues, percentage of variance and cumulative obtained through PCA.

Principal Component Number	Eigenvalue	Percentage of Variance (%)	Cumulative (%)
1	4.78652	53.1836	53.1836
2	2.86274	31.80819	84.9918
3	0.70691	7.85458	92.84638
4	0.24717	2.74638	95.59276
5	0.18505	2.05616	97.64891
6	0.10686	1.18739	98.8363
7	0.06212	0.69017	99.52647
8	0.02893	0.3215	99.84797
9	0.01368	0.15203	100